Supplement of Atmos. Chem. Phys., 19, 5571–5587, 2019
https://doi.org/10.5194/acp-19-5571-2019-supplement

Atmospheric Chemistry and Physics
Open Access
EGU

Supplement of

Insights into the morphology of multicomponent organic and inorganic aerosols from molecular dynamics simulations

Katerina S. Karadima et al.

Correspondence to: Spyros N. Pandis (spyros@chemeng.upatras.gr)

S1 Additional OPLS force field parameters

The all–atom Optimized Potentials for Liquid Simulations (OPLS) forcefield was adopted in our simulations (Jorgensen and Tirado-Rives, 1988). The types and the functional forms of the energies that contribute to the total potential energy, as well the corresponding parameters for the molecules simulated here are available in the Supplementary Information of Karadima et al. (2017). The parameters provided there were also used for MBTCA, *n*-eicosane, and *n*-tetracosane. Additional parameters are reported in Table S1.

Table S1. Forcefield parameter values for the torsional (dihedral angles) interactions not included in Karadima et al. (2017).

Dihedral angle type	V_1 (kcal mol^{-1})	V_2 (kcal mol^{-1})	V_3 (kcal mol^{-1})
C-CT-CT-CT, RCOOH	-2.060	-0.313	0.315
C-CT-CT-C, RCOOH	-0.550	0.000	1.000

Note: For notation, see the Supplementary Information of Karadima et al. (2017).

S2 Particle volume discretization

The surface area of an ellipsoid with semi–axes a, b, c is described by:

$$\frac{x^2}{a^2}+\frac{y^2}{b^2}+\frac{z^2}{c^2}=1. \tag{S0}$$

The volume of such an ellipsoid is given by:

$$V_{\text{total}}=\frac{4\pi}{3}abc. \tag{S0}$$

The space occupied by the ellipsoid can be split into *n* successive and self–similar sub–ellipsoids (i.e., ellipsoids that have the same eccentricities as the original) of equal volume, each one described by the following equation:

$$\frac{x^2}{\left(\lambda_i a\right)^2}+\frac{y^2}{\left(\lambda_i b\right)^2}+\frac{z^2}{\left(\lambda_i c\right)^2}=1. \tag{S0}$$

The parameter λ_i is given by:

$$\lambda_i=\sqrt[3]{\frac{i}{n}} \tag{S0}$$

so that the sum of the volumes of the *n* sub–ellipsoids is equal to the total volume of the initial ellipsoid, $\sum_{i=1}^{n}V_i=V_{\text{total}}$. Then, we also have that $V_{i+1}-V_i=\frac{V_{\text{total}}}{n}$. Indeed, the volume enclosed by each sub–ellipsoid is

$$V_i=\frac{4\pi}{3}\left(\sqrt[3]{\frac{i}{n}}a\right)\left(\sqrt[3]{\frac{i}{n}}b\right)\left(\sqrt[3]{\frac{i}{n}}c\right)=\frac{i}{n}\left(\frac{4\pi}{3}abc\right)=\frac{i}{n}V_{\text{total}} \tag{S0}$$

thus,

$$V_{i+1} - V_i = \frac{i+1}{n} V_{\text{total}} - \frac{i}{n} V_{\text{total}} = \frac{V_{\text{total}}}{n}. \qquad \text{(S0)}$$

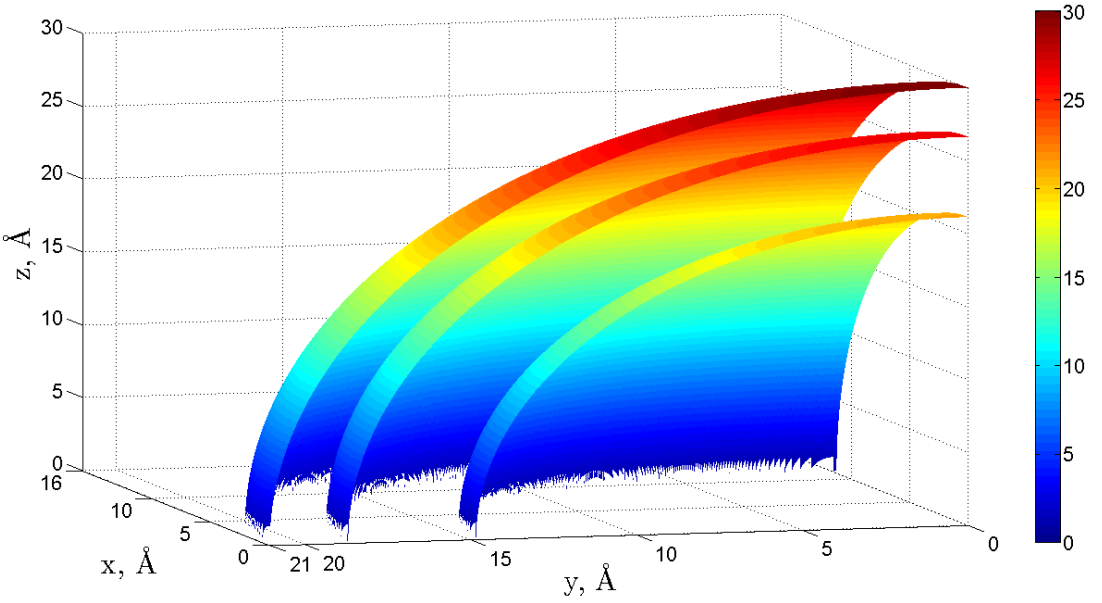

Figure S1. Schematic representation of one eighth of an ellipsoidal nanoparticle formed in the course of our MD simulations with semi–axes equal to 16, 21 and 30 Å, and its division in the three characteristic domains defined in the text as we move from its centre outwards: the core, the intermediate ring, and the surface.

In the case of the ellipsoidal nanoparticles formed in the course of our MD simulations, we divide the space occupied by them in three sub–regions (Fig. S1). The first corresponds to 35 % of the total particle volume around the center of the ellipsoid (the core), the second corresponds to another 35 % of the total particle volume covering the area right after the core and defines the intermediate (ring/doughnut–like) region of the nanoparticle, and the third corresponds to the last 30 % of the total particle volume starting after the intermediate ring and corresponds to the outer area of the nanoparticle (its surface).

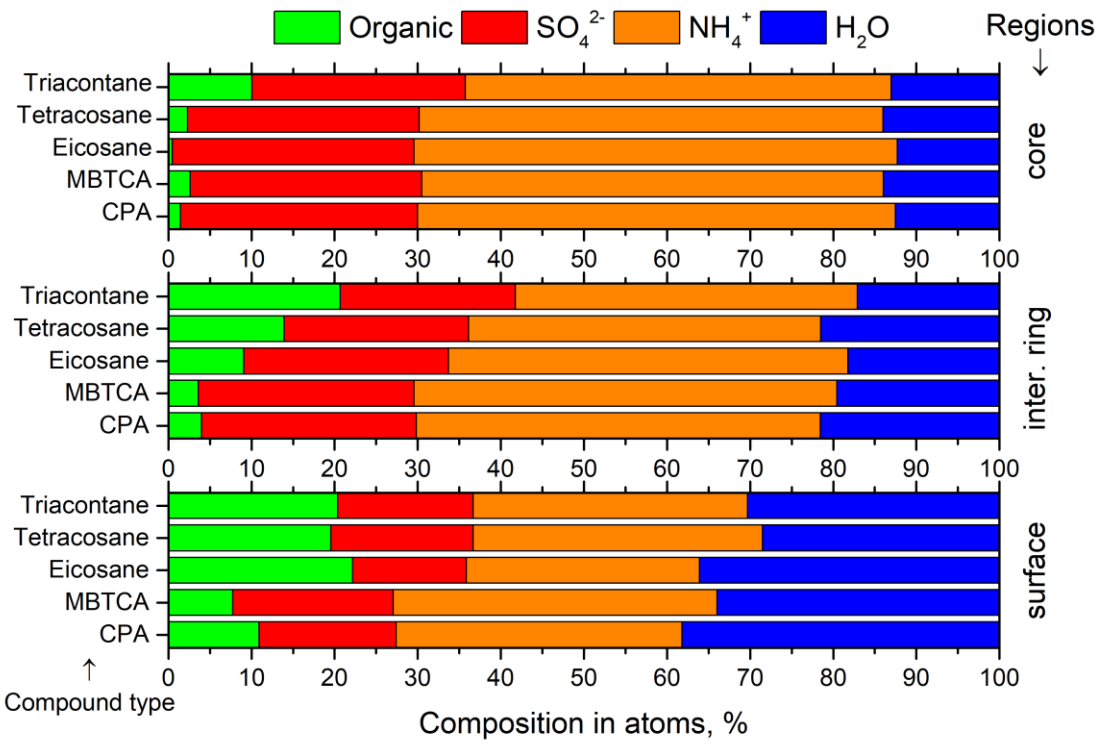

Figure S2. Composition of the three particle regions of the simulated nanoparticles containing (a) CPA, (b) MBTCA, (c) *n*-eicosane, (d) *n*-tetracosane, and (e) *n*-triacontane. Conditions: low organic mass content and low water mass fraction.

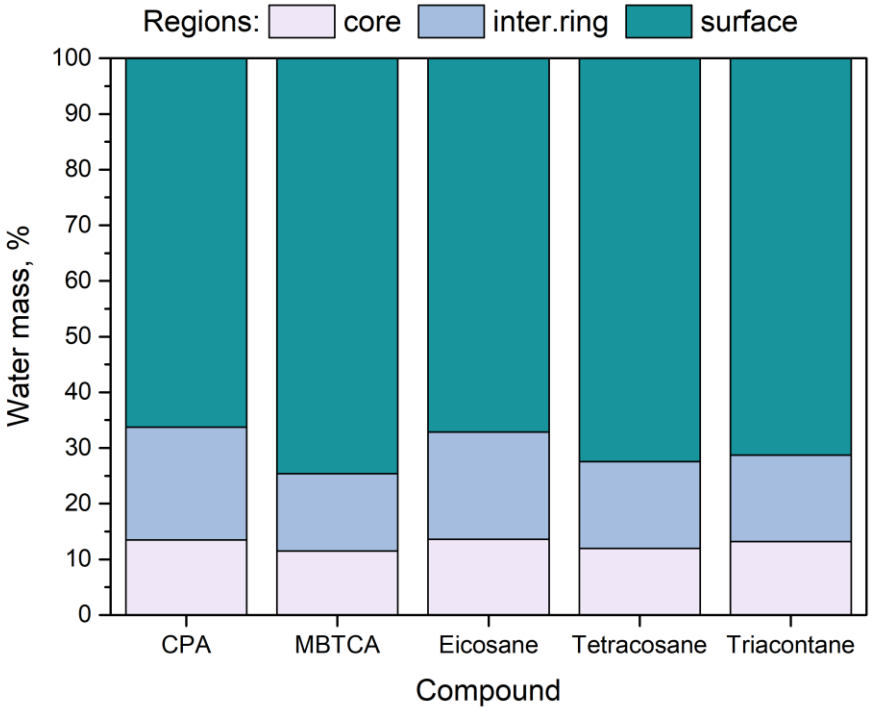

Figure S3. Percentage of water molecules in the three regions (core, intermediate ring, outer surface) of the simulated nanoparticles containing CPA, MBTCA, *n*-eicosane, *n*-tetracosane, and *n*-triacontane. Conditions: dry organic mass content 7–14 %, RH 40 %.

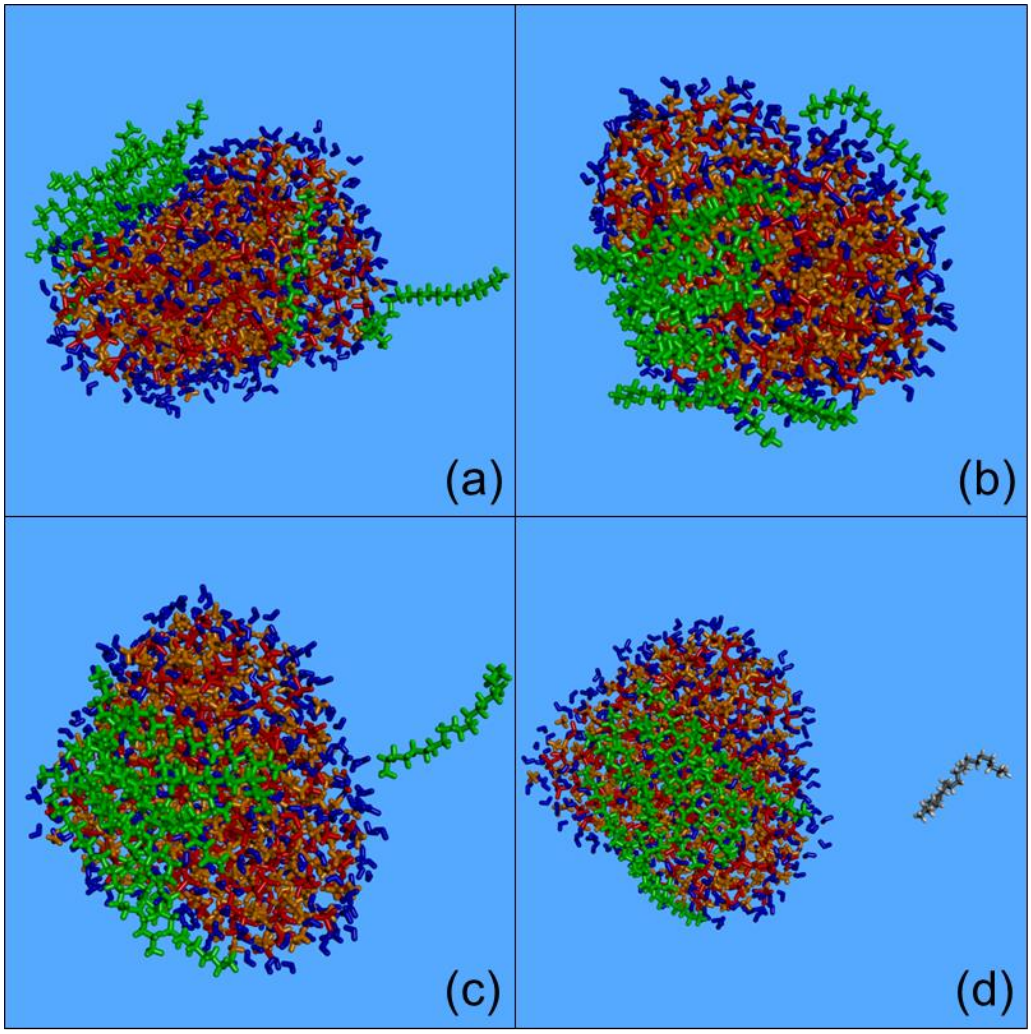

Figure S4. Typical snapshots of a simulated nanoparticle composed of 10 *n*-eicosame molecules (green, or dark grey for C atoms and light grey for H atoms), 200 sulfate ions (red), 400 ammonium ions (orange) and around 392 water molecules (blue), taken at (a) 46.20 ns, (b) 59.14 ns, (c) 59.15 ns, and (d) 59.16 ns. During this simulation, two *n*-eicosane molecules were close to migrating to the gas phase. Finally, only the *n*-eicosane molecule depicted in (b–d) abandoned the particulate phase (c–d) and remained in the gas phase for the rest of the simulation.

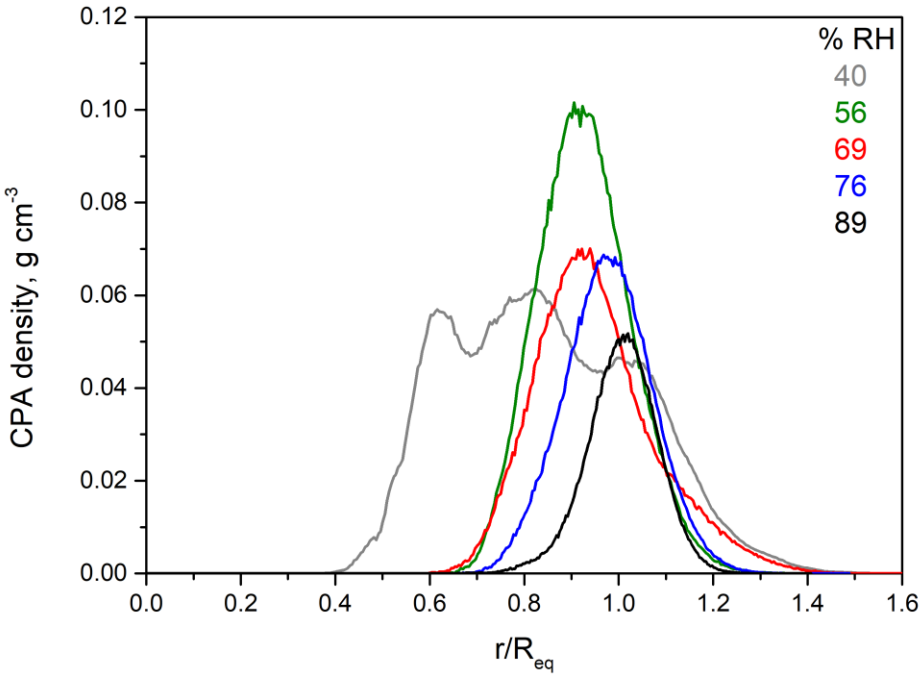

Figure S5. Local CPA density in the nanoparticles as a function of radial distance r/R_{eq} from their centre–of–mass, for various RH levels and low CPA mass content (7 % dry).

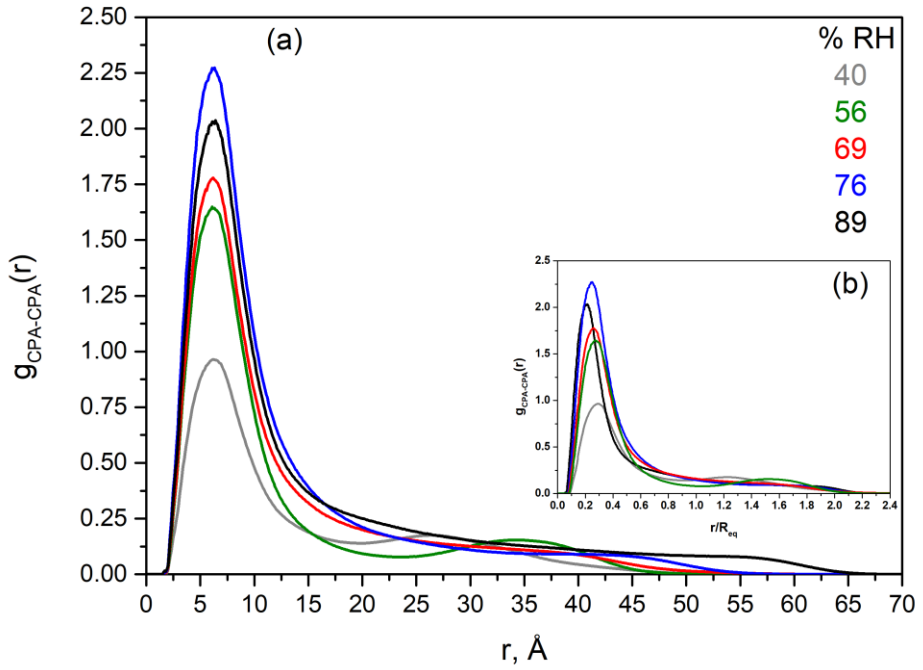

Figure S6. Radial pair correlation function of CPA molecules in the formed nanoparticles as a function of (a) radial distance r (b) r/R_{eq} under various RH levels and 7 % dry CPA mass content.

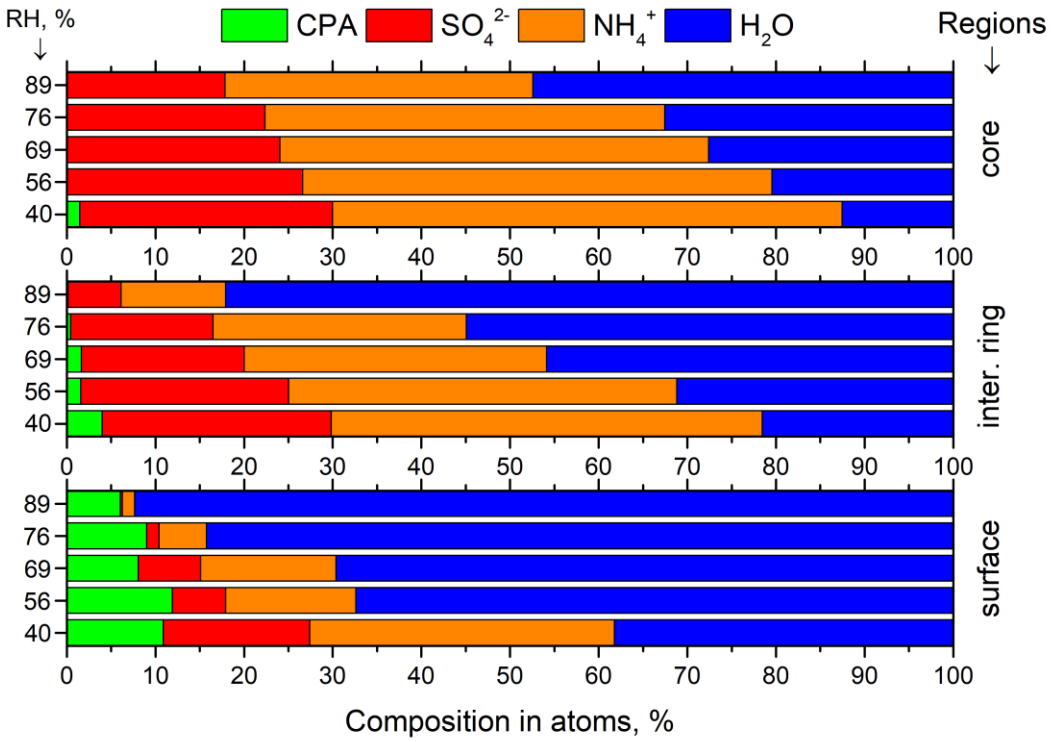

Figure S7. Representation of the composition of the three particle regions of the simulated nanoparticles containing CPA, under various RH levels and low organic mass fraction.

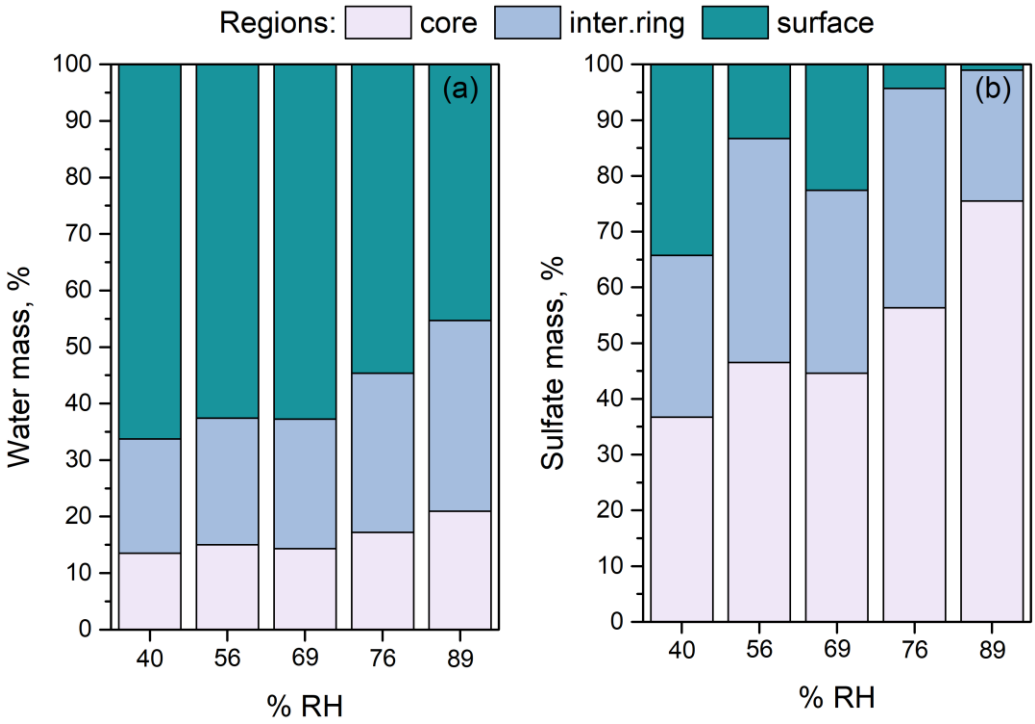

Figure S8. Percentage of (a) water molecules and (b) sulfate ions in the three regions (core, intermediate ring, outer surface) of the simulated nanoparticles containing CPA with low organic mass content (7 %), as a function of RH.

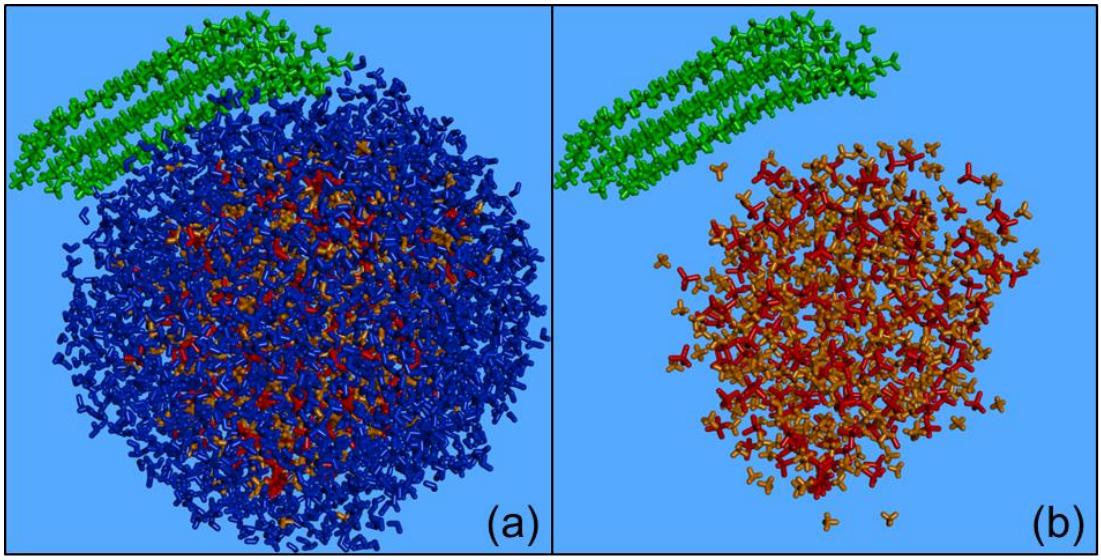

Figure S9. Snapshots from the simulation of a nanoparticle containing 14 % *n*-triacontane at 89 % RH (a) including and (b) omitting water molecules. Colour notation: green for *n*-triacontane, red for sulfate, orange for ammonium and blue for water.

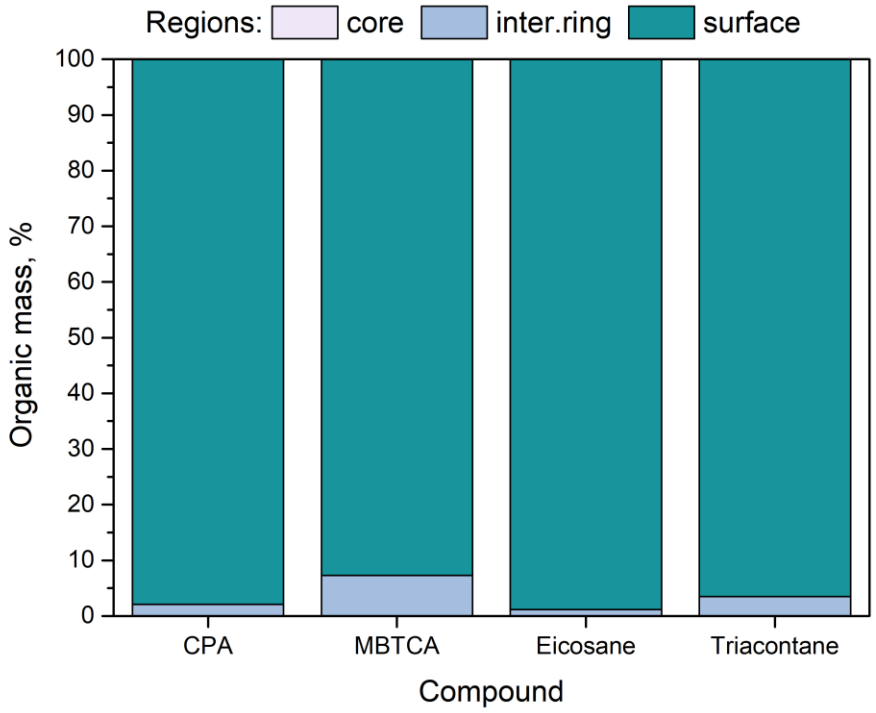

Figure S10. Percentage of CPA, MBTCA, *n*-eicosane and *n*-triacontane in the three regions (core, intermediate ring, outer surface) of the simulated nanoparticles at 89 % RH and low organic mass content (7–14 % dry).

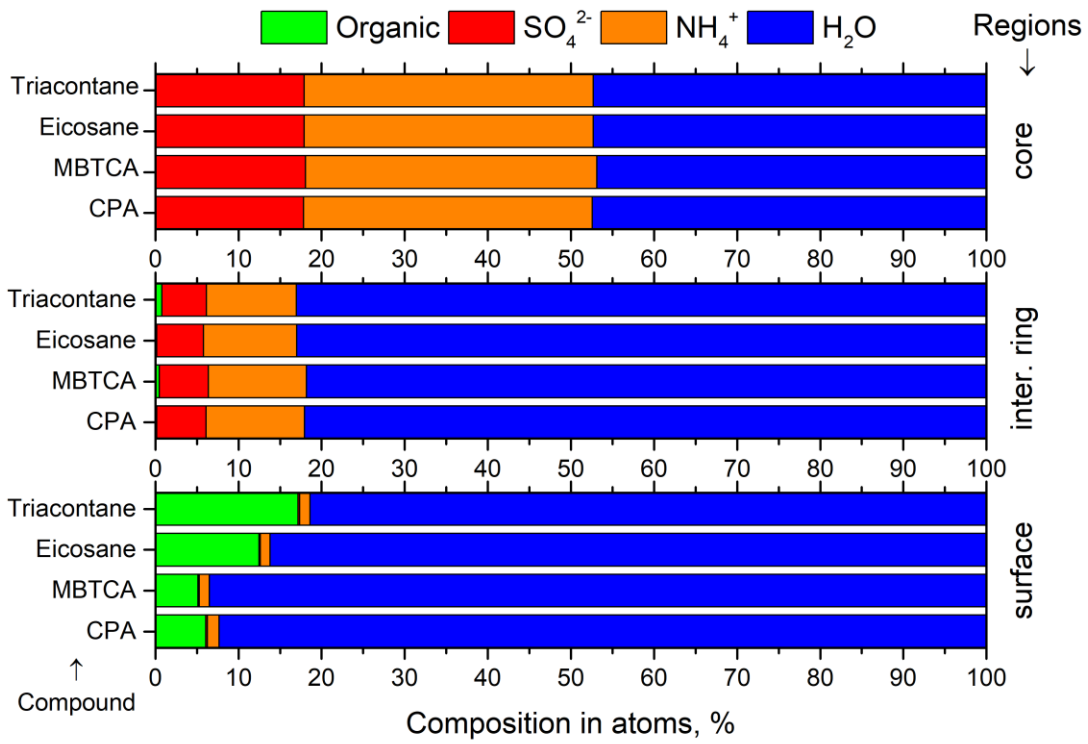

Figure S11. Composition of the three particle regions of the simulated nanoparticles containing CPA, MBTCA, *n*-eicosane and *n*-triacontane at 89 % RH and low organic mass fraction (7–14 %).

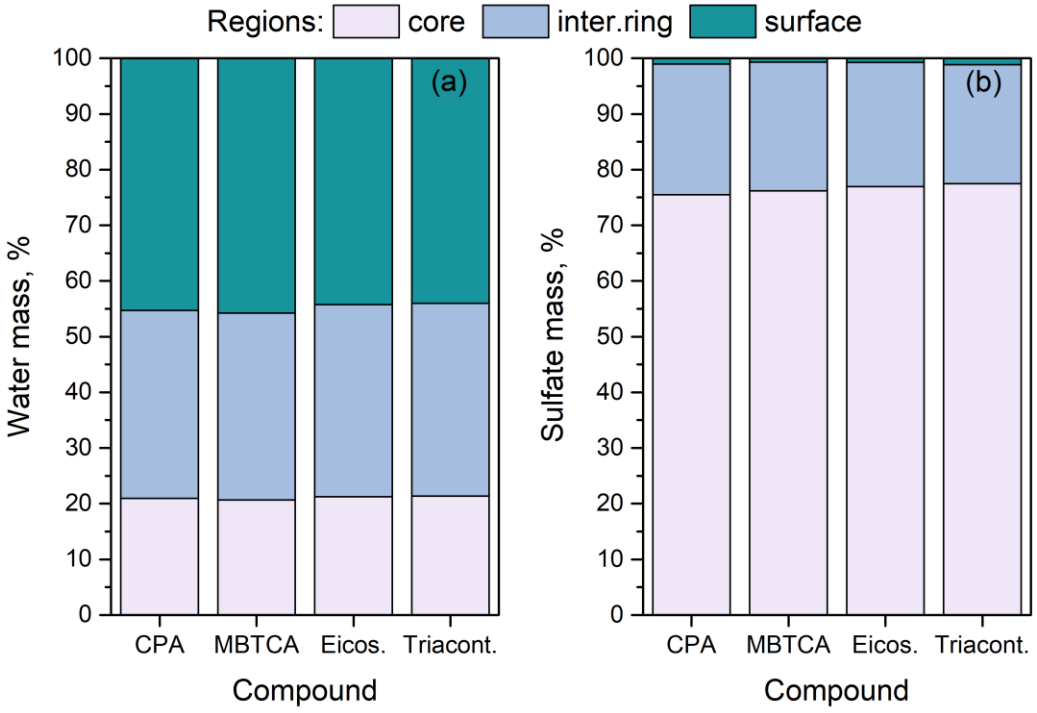

Figure S12. Percentage of (a) water molecules and (b) sulfate ions in the three regions (core, intermediate ring, surface) of the simulated nanoparticles containing CPA, MBTCA, *n*-eicosane and *n*-triacontane at 89 % RH and low organic mass content (7–14 % dry).

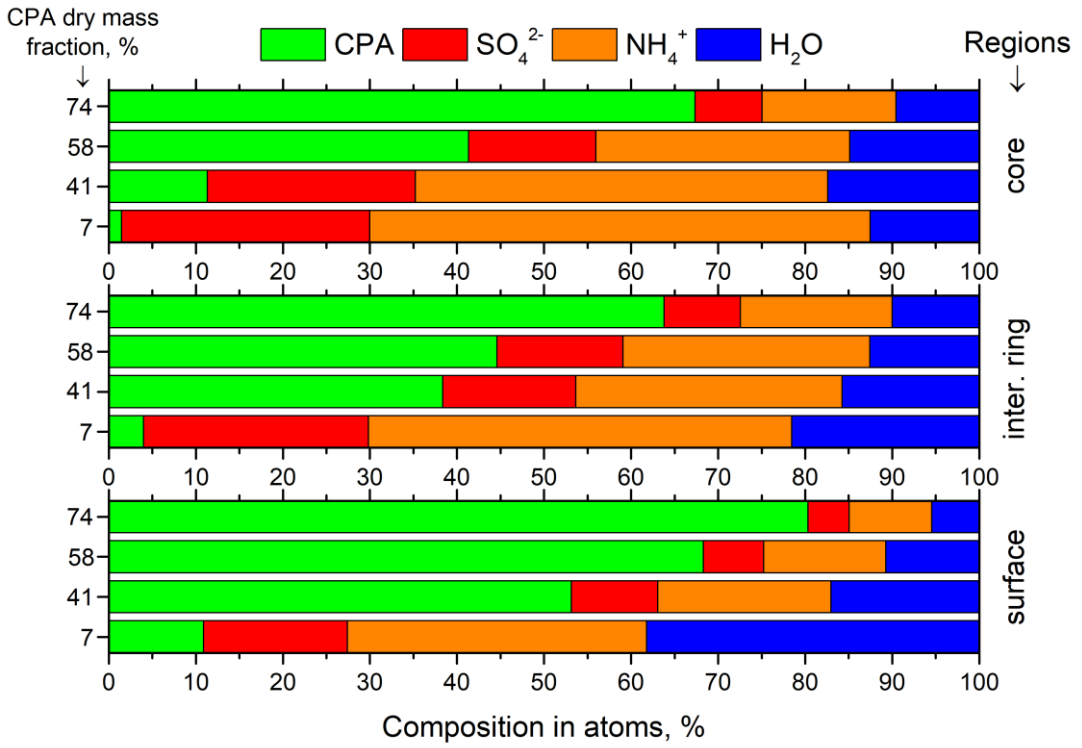

Figure S13. Composition of the three particle regions of the simulated nanoparticles containing CPA, under various organic mass fractions and low relative humidity.

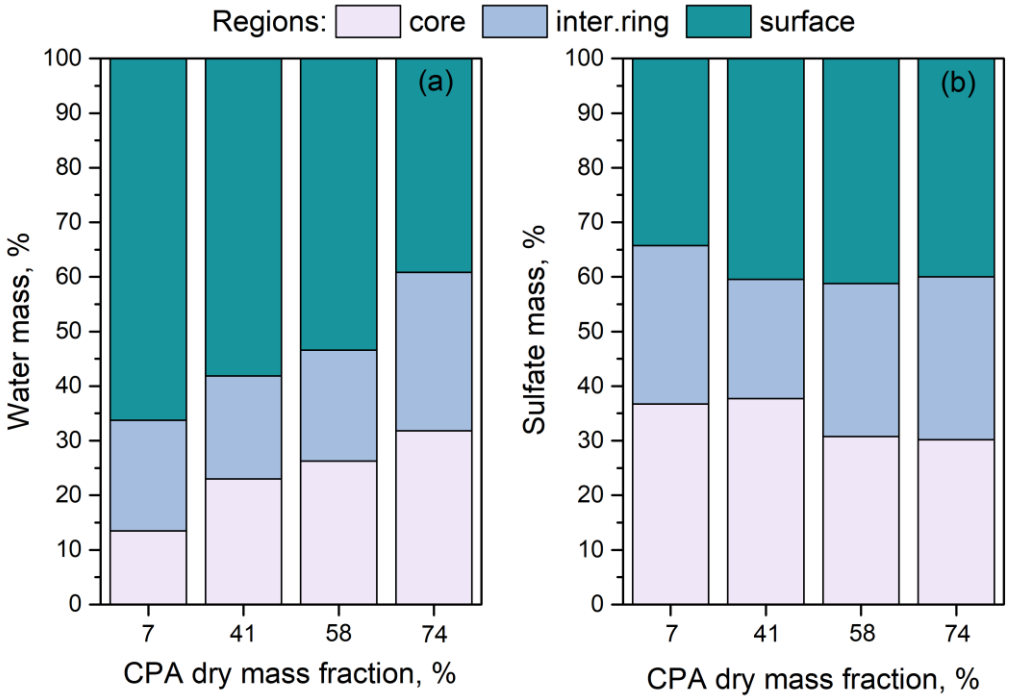

Figure S14. Percentage of (a) water molecules and (b) sulfate ions in the three regions (core, intermediate ring, outer surface) of the simulated nanoparticles for 41, 58, and 74 % dry organic mass content and comparison with the particle with 7 % dry CPA mass content, at low water content for all particles.

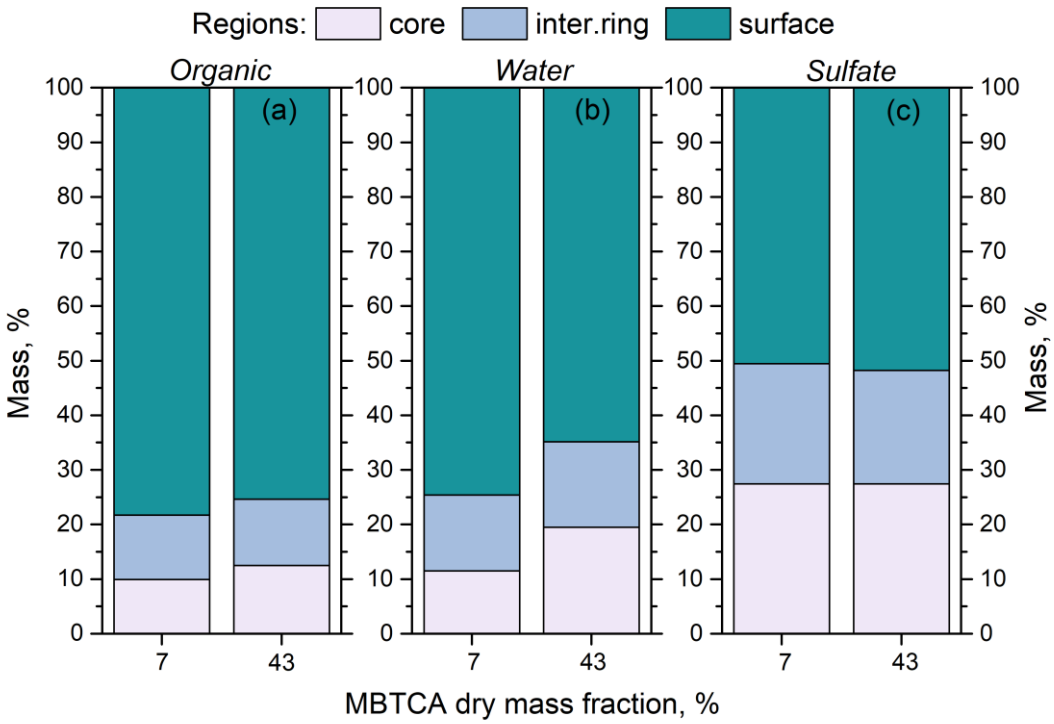

Figure S15. Percentage of (a) MBTCA molecules, (b) water molecules and (c) sulfate ions in the three regions (core, intermediate ring, outer surface) of the simulated nanoparticles for 7 and 43 % dry MBTCA mass fraction, at low water content.

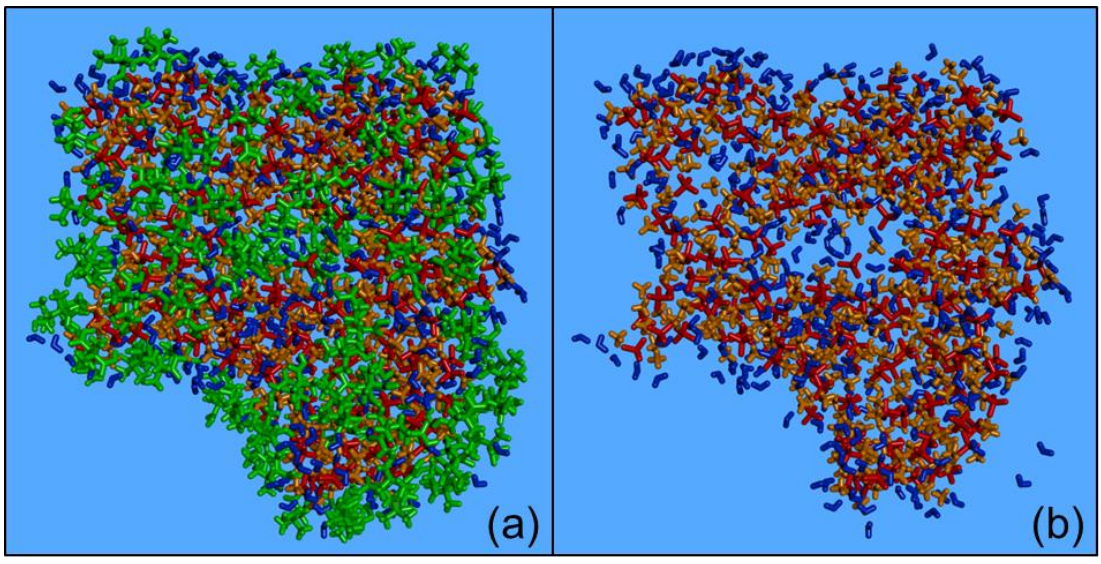

Figure S16. Snapshots from the simulation of a nanoparticle containing MBTCA (43 % dry) at 40 % RH (a) including and (b) omitting MBTCA molecules. Colour coding: green for MBTCA, red for sulfate, orange for ammonium and blue for water.

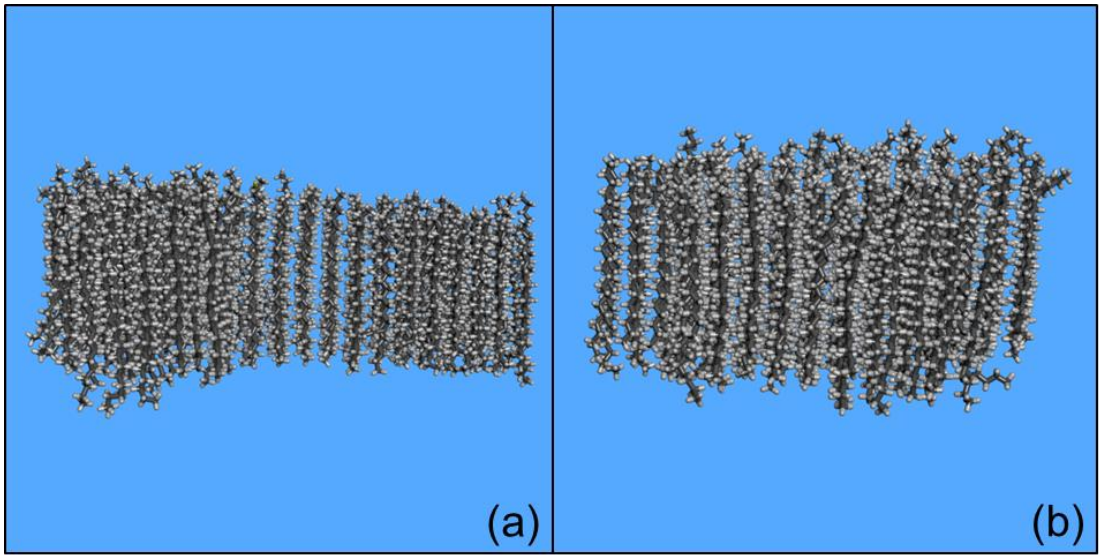

Figure S17. Atomistic snapshot of a nanoparticle containing *n*-eicosane (63 % dry) at 76 % RH. Inorganic species are omitted and only alkane chains are shown using two different views, (a) and (b). Colour notation: dark grey for carbons and light grey for hydrogens.

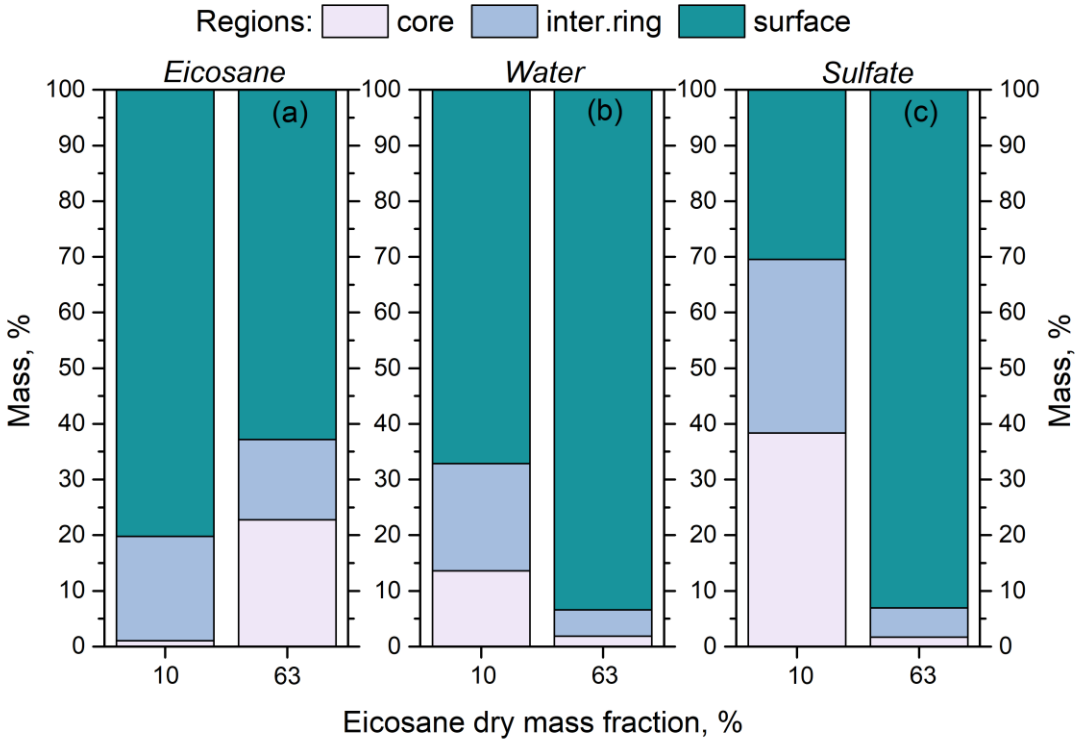

Figure S18. Percentage of (a) *n*-eicosane molecules, (b) water molecules, and (c) sulfate ions in the three regions (core, intermediate ring, outer surface) of the simulated nanoparticles for *n*-eicosane–containing nanoparticles with 10 and 63 % dry mass fractions at 40 and 76 % RH, respectively.

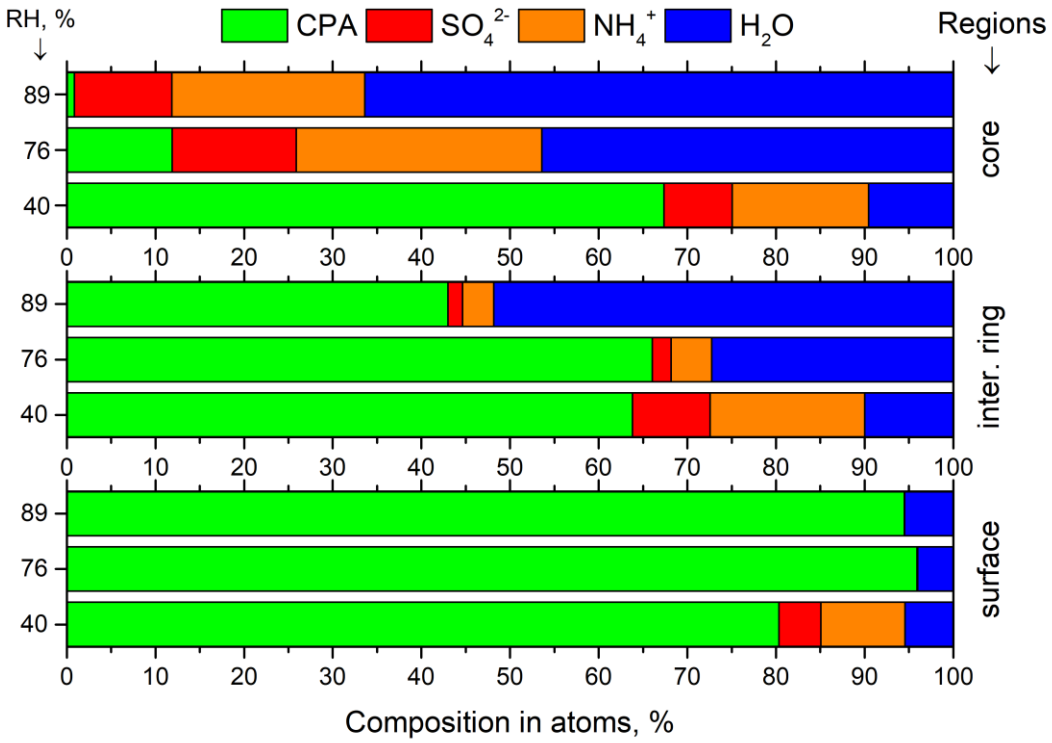

Figure S19. Composition of the three particle regions of the simulated nanoparticles containing 74 % CPA, as a function of RH.

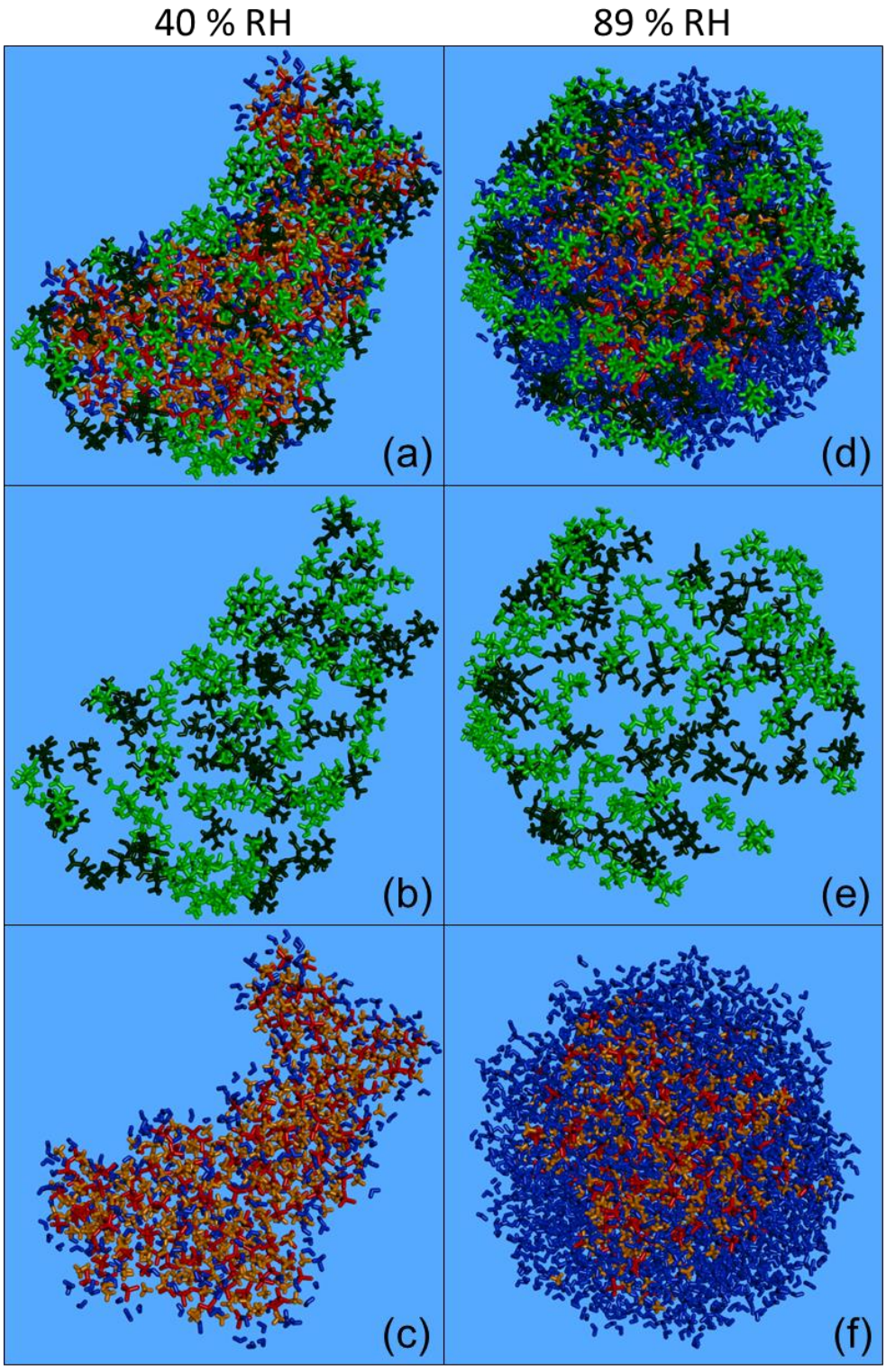

Figure S20. Characteristic snapshots from the MD simulation of the nanoparticles containing (dry mass fraction) 20 % CPA and 23 % MBTCA (a) at 40 % RH, (b) at 40 % RH including only organic molecules, (c) at 40 % RH omitting organic molecules, (d) at 89 % RH, (e) at 89 % RH including only organic molecules, and (f) at 89 % RH omitting organic molecules. Colour coding: green for CPA, dark green for MBTCA, red for sulfate, orange for ammonium, and blue for water.

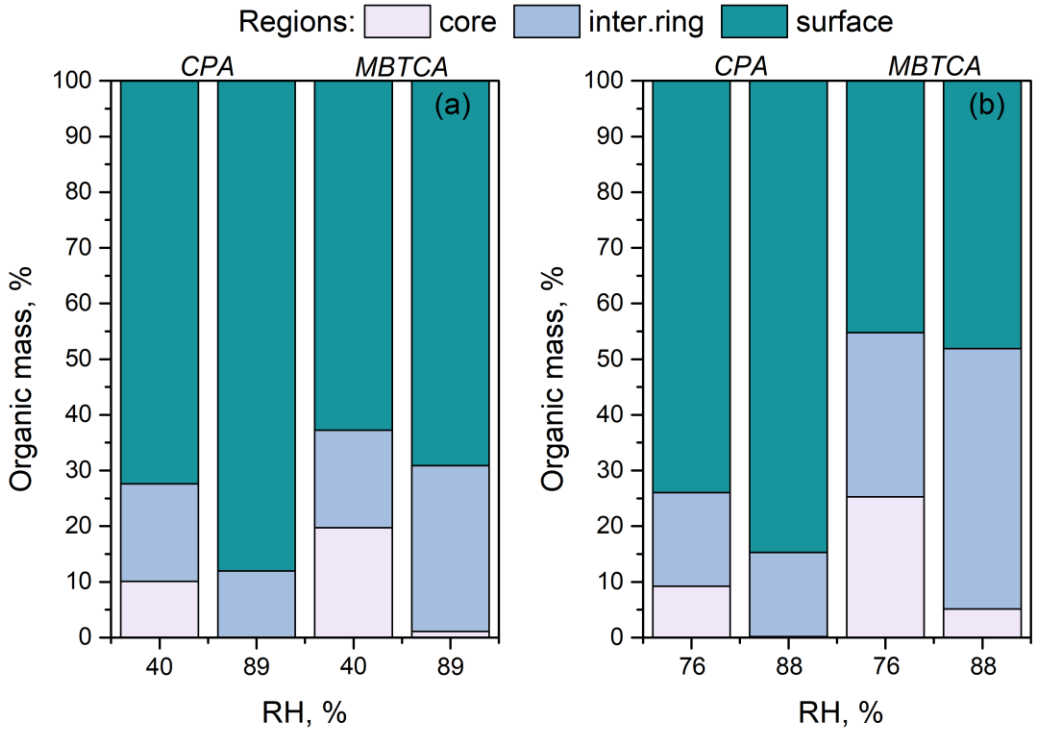

Figure S21. Percentage of CPA and MBTCA molecules in the three regions (core, intermediate ring, outer surface) of the particles containing mixtures of CPA and MBTCA with (a) 43 and (b) 75 % dry total mass fractions, under different RH.

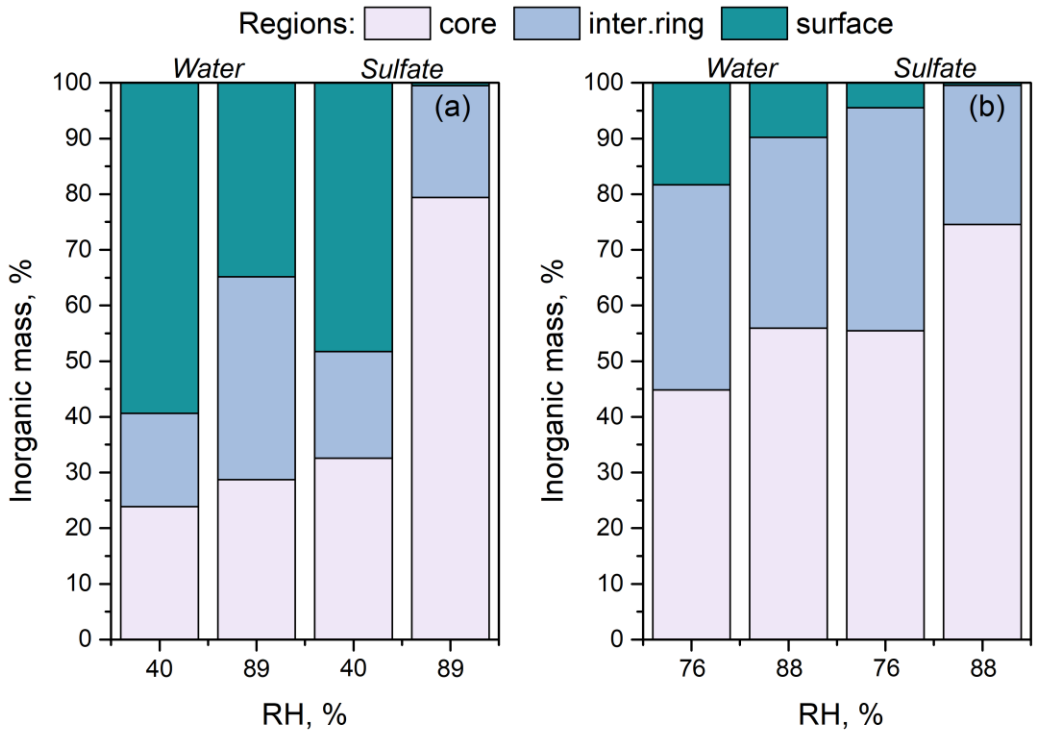

Figure S22. Percentage of water molecules and sulfate ions in the three regions (core, intermediate ring, outer surface) of the simulated nanoparticles containing mixtures of CPA and MBTCA with (a) 43 and (b) 75 % dry total mass fractions, as a function of RH.

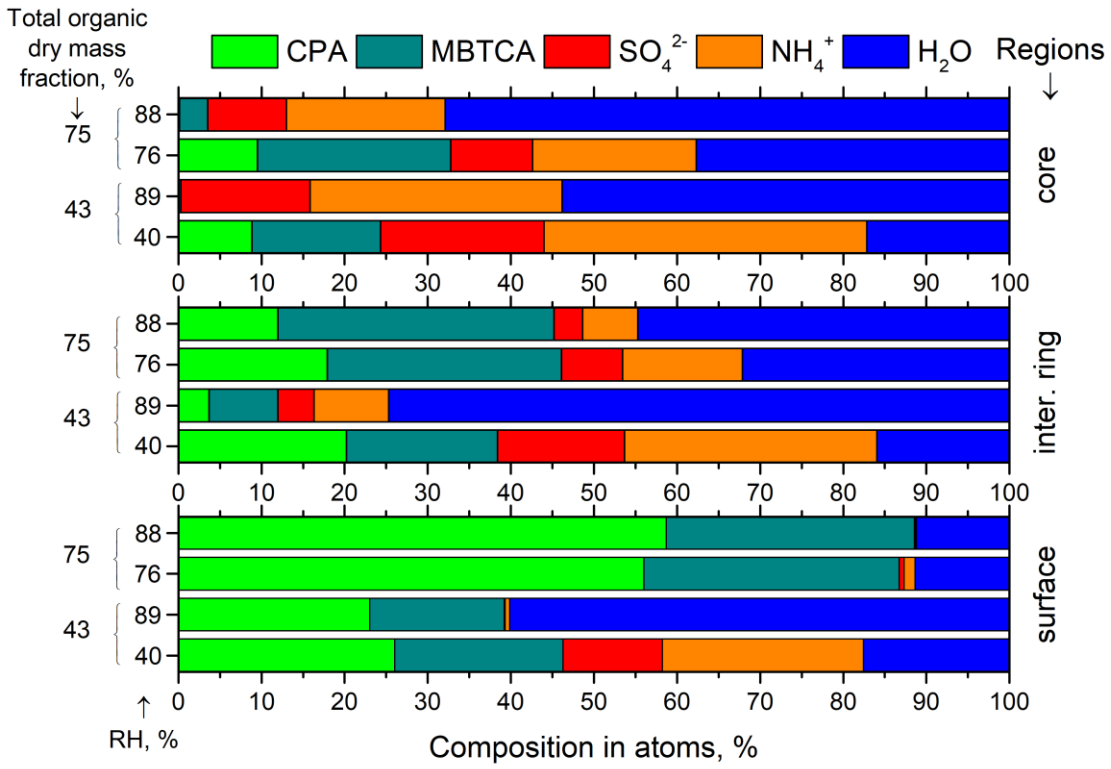

Figure S23. Composition of the three particle regions of the simulated nanoparticles containing 43 and 75 % total organic mass composed of CPA and MBTCA, at various RH.

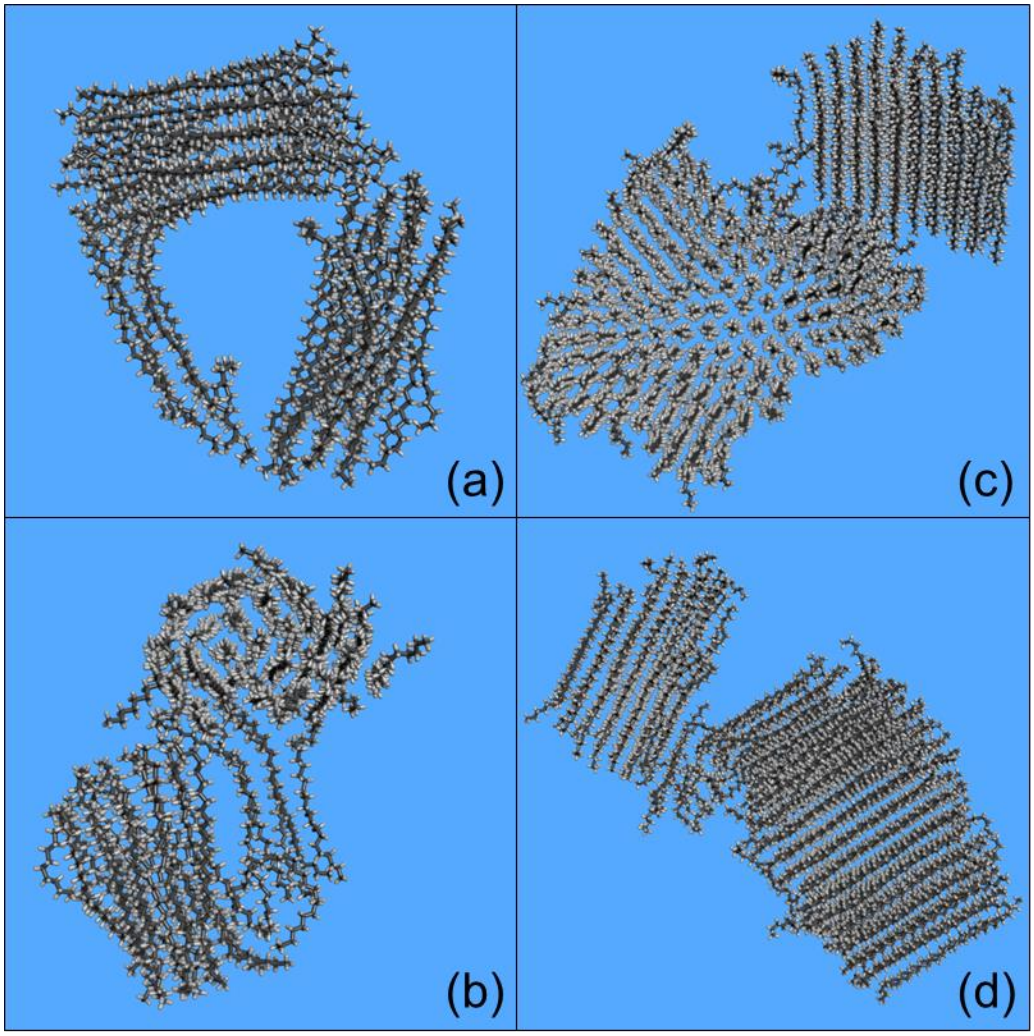

Figure S24. Characteristic simulation snapshots of nanoparticles containing CPA and *n*-triacontane with (a)–(b) 53 % dry total organic mass fractions and (c)–(d) 82 % organics, under low RH. Inorganic species and CPA molecules are omitted and only alkane chains are depicted. Two different views of each particle are shown. Colour notation: dark grey for carbons and light grey for hydrogens.

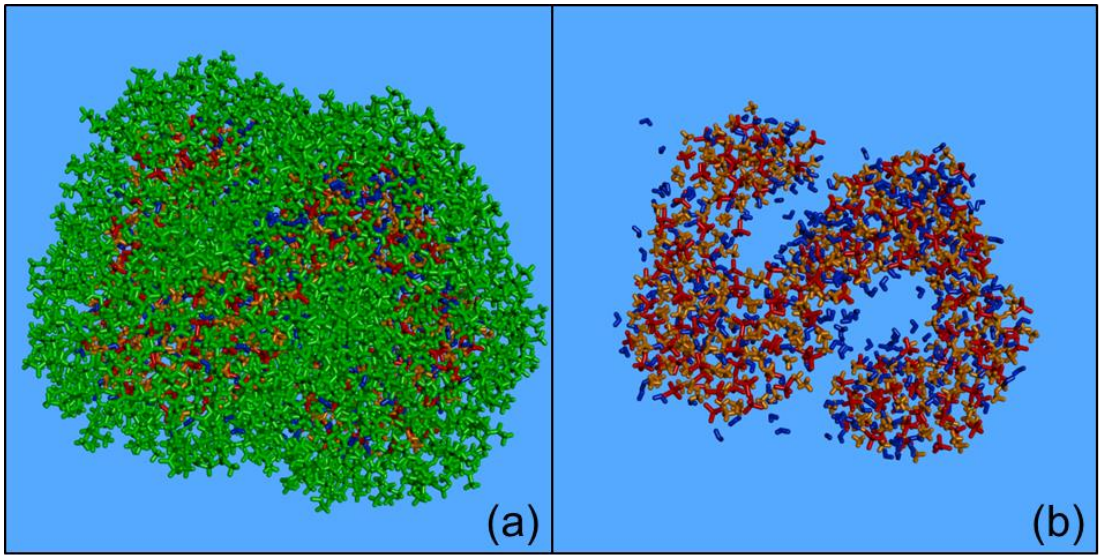

Figure S25. Snapshots of the nanoparticle that contains 74 % CPA at 39 % RH, after being simulated for 30 ns at 350 K (a) including and (b) omitting CPA molecules. Colour notation: green for CPA, red for sulfate, orange for ammonium and blue for water.

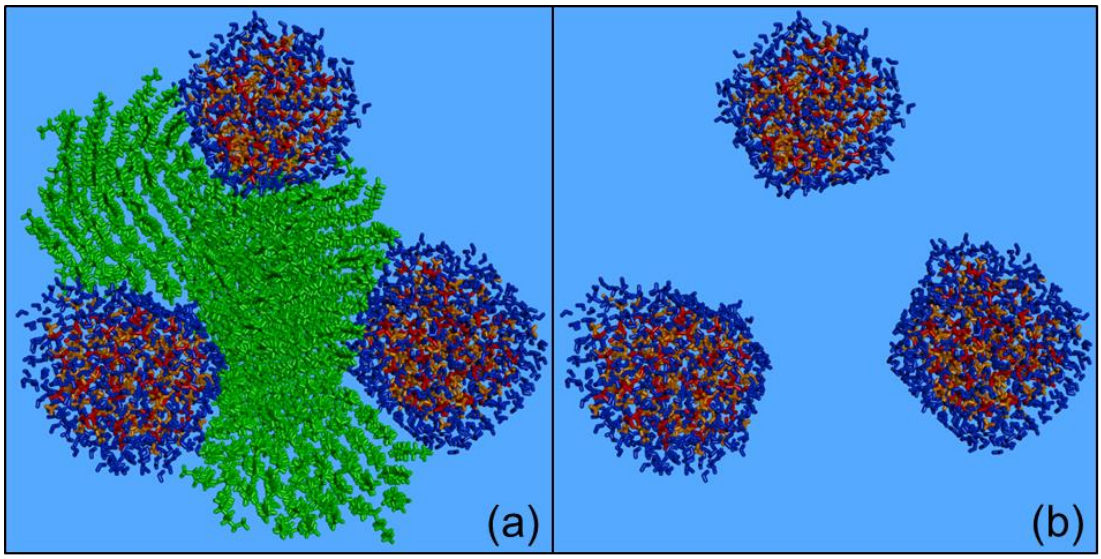

Figure S26. Characteristic snapshot from the second MD simulation of the nanoparticle containing n-eicosane (63 % dry) at 68 % RH, (a) including and (b) omitting n-eicosane molecules. Colour coding: green for n-eicosane, red for sulfate, orange for ammonium, and blue for water.

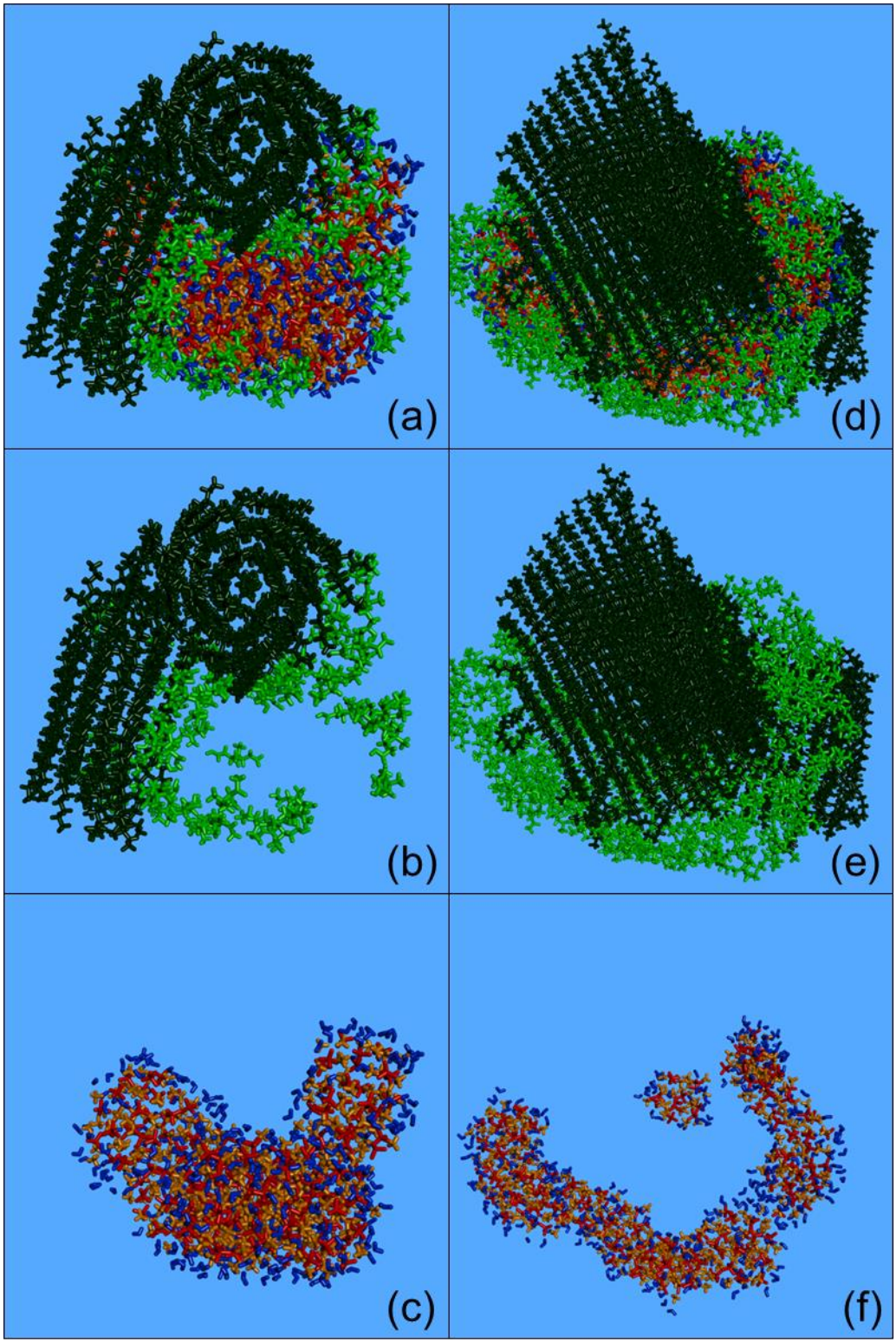

Figure S27. Characteristic snapshots from the second MD simulations of the two nanoparticles containing CPA and n-triacontane at around 40 % RH: (a) with 53 % dry organic content, (b) with 53 % dry organic content including only organic molecules, (c) with 53 % dry organic content omitting organic molecules, (d) with 82 % dry organic content, (e) with 82 % dry organic content including only organic molecules, and (f) with 82 % dry organic content omitting organic molecules. Colour coding: green for CPA, dark green for n-triacontane, red for sulfate, orange for ammonium, and blue for water.

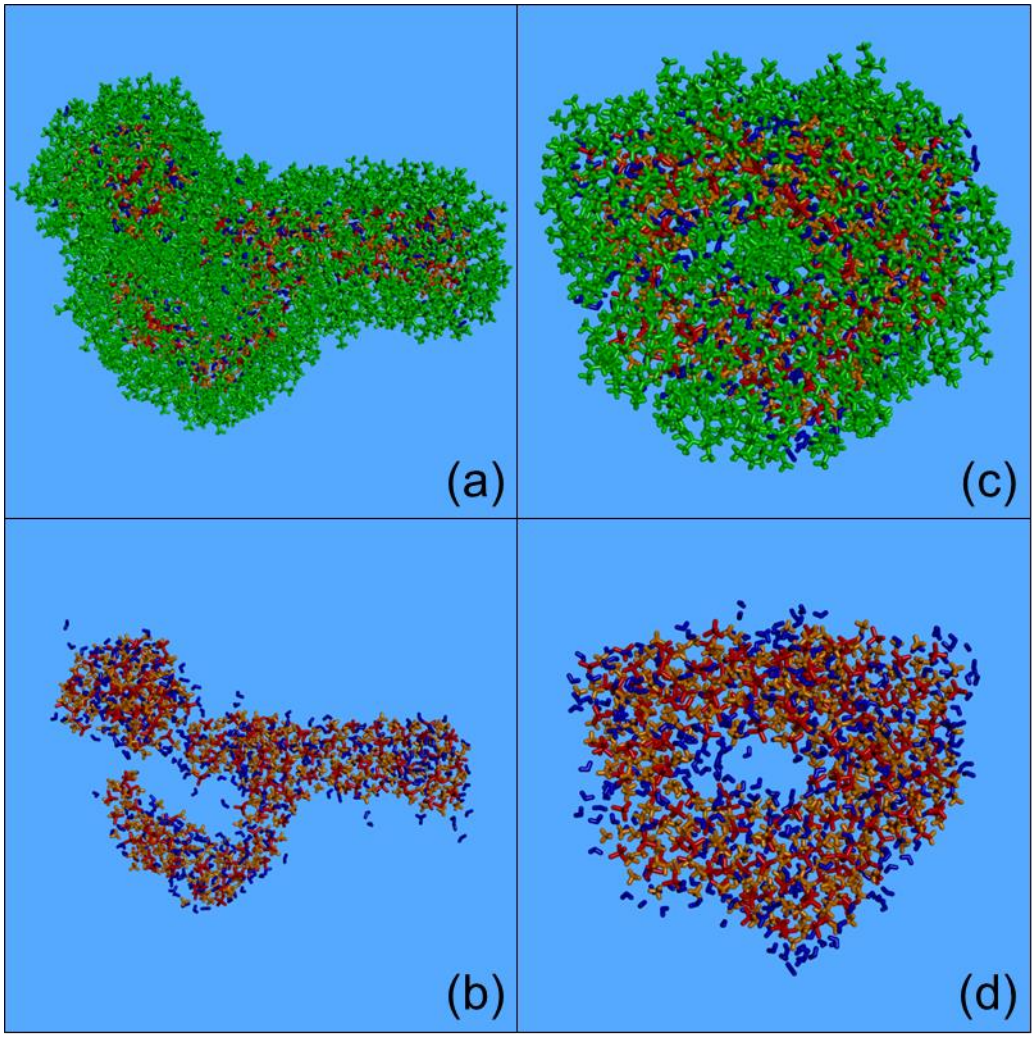

Figure S28. Characteristic snapshots from: (a) the second MD simulation of the nanoparticle containing CPA (74 % dry) at 39 % RH including all molecules, (b) the second MD simulation of the nanoparticle containing CPA (74 % dry) at 39 % RH omitting CPA molecules, (c) the extended MD simulation of the nanoparticle containing CPA (58 % dry) at 40 % RH including all molecules, and (d)) the extended MD simulation of the nanoparticle containing CPA (58 % dry) at 40 % RH omitting CPA molecules. Colour coding: green for CPA, red for sulfate, orange for ammonium, and blue for water.